

## Anisotropic Spin Correlations in the Zn-Mg-Ho Icosahedral Quasicrystal

Taku J. Sato,<sup>1</sup> Hiroyuki Takakura,<sup>1,2</sup> An Pang Tsai,<sup>1</sup> and Kaoru Shibata<sup>3</sup>

<sup>1</sup>National Research Institute for Metals, Tsukuba 305-0047, Japan

<sup>2</sup>CREST, Japan Science and Technology Corporation, Kawaguchi, Saitama, Japan

<sup>3</sup>Institute for Materials Research, Tohoku University, Sendai, Japan

(Received 26 March 1998)

Neutron scattering experiments have been performed on the Zn-Mg-Ho icosahedral quasicrystal using powder and single-crystalline samples. In contrast to a previous Letter [Charrier *et al.*, Phys. Rev. Lett. **78**, 4637 (1997)], the magnetic long-range order could not be detected in the icosahedral quasicrystal. It instead exhibits highly anisotropic diffuse scattering, which appears as satellite ridges of intense nuclear Bragg reflections, running parallel to the fivefold axis. The result suggests that quasi-five-dimensional spin correlations develop on a six-dimensional hypercubic lattice. [S0031-9007(98)06916-6]

PACS numbers: 75.50.Lk, 61.44.Br, 75.40.-s

Quasicrystals (QCs) are characterized by sharp Bragg reflections with a point-symmetry that is prohibited in a periodic lattice, such as fivefold or tenfold symmetry. To account for the Bragg reflections and point-symmetry at once, quasiperiodicity was proposed and today is widely accepted [1]. This quasiperiodicity can be regarded as a projection of a periodic structure in a higher-dimensional virtual space into the three-dimensional (3D) real space. Owing to the novel structure, physical properties of the quasiperiodic systems are quite intriguing to study [2]. Icosahedral quasicrystal (i-QC) is one realization of such quasiperiodic systems, which can be described as a projection of a six-dimensional (6D) hypercubic lattice into the 3D space. It shows twofold (2f), threefold (3f), and fivefold (5f) symmetric axes. The i-QC can most easily be obtained in real alloys, e.g., Al-Pd-Mn [3] or Al-Li-Cu [4], and some of them can be grown in a macroscopic size. Thus, various physical properties have been investigated using i-QC, for example, electrical resistivity [5] and phonon dispersion relation [6]. They show almost no direction dependence, and this isotropic behavior is thought to originate from the high point-symmetry of the i-phase.

Recently, i-QC was found in the Zn-Mg-RE (RE: rare earth) system [7]. Since this system has localized 4f magnetic moments (or atomic spins) on the RE sites, it provides an opportunity to study magnetism on the quasiperiodic lattice. To date, the neutron powder diffraction was performed and suggested a coexistence of the magnetic short-range order (SRO) and long-range order (LRO) at low temperatures, such as  $T < T_N \approx 7$  K for RE = Ho [8]. The LRO was shown to have a wave vector of  $\vec{q}_{6D} = (\frac{1}{2}00000)_{6D}$  and was named as *quasimag-netism*. (Suffix "6D" indicates that the vector is defined with the 6D reciprocal lattice bases [9].) If the LRO really existed, this could be the first experimental evidence of a quasiperiodic spin structure with an anisotropy in the  $\vec{q}_{6D}$  vector. However, the magnetic susceptibility shows no anomaly at  $T_N$  but instead exhibits a spin-glass-like transition at lower temperatures, for example,  $T_{SG} \approx 2$  K

for RE = Ho [10,11]. This rather indicates that spins are paramagnetic above  $T_{SG}$  and randomly freeze at this temperature. Hence, the two results are contradicting. Recent metallographic investigations show that the i-QC has an almost stoichiometric composition of  $Zn_{60}Mg_{30}RE_{10}$  [12]. However, the previous magnetic experiments used  $Zn_{50}Mg_{42}RE_8$  samples, which can probably be contaminated by several crystalline phases. Therefore reexamination of a single-phased sample is necessary. In this sense, a single crystal study is much preferable since it is, in principle, a perfect single phase. In addition, it gives information on the  $\vec{Q}$ -direction dependence.

In the present study, we have performed neutron scattering experiments on powder and single crystalline samples of the Zn-Mg-Ho system. We selected RE = Ho because the most distinct LRO was reported for Ho. In our results, the LRO could not be detected, whereas highly anisotropic diffuse scattering was observed in the single i-phased sample. As far as we know, this is the first observation of the clear anisotropy in physical properties. From the  $\vec{Q}$  dependence, the diffuse scattering should be regarded as quasi-five-dimensional spin correlations defined in the 6D space.

The Zn-Mg-Ho powder samples were prepared by melting constituent elements. The samples were characterized by scanning and transmission electron microscopies (SEM and TEM) and x-ray diffraction. The 0.5 cm<sup>3</sup> single crystal of i-QC was obtained by the Bridgman method. Details of the crystal growth were published elsewhere [13]. Neutron diffraction experiments were performed at the triple-axis spectrometer ISSP-GPTAS installed at JRR-3M, JAERI (Tokai), operated in the double-axis configuration. Collimations of 40'-80'-40' or 40'-80'-80' were employed. Incident neutrons of  $k_i = 2.67 \text{ \AA}^{-1}$  were selected by a vertically focusing pyrolytic graphite (PG) monochromator, and second harmonics is eliminated by the PG filter. In the single-crystal experiment, the scattering plane was chosen normal to a 2f axis, so that the plane contains all the 2f, 3f, and 5f axes.

First of all, we examined the microstructure of the  $\text{Zn}_{50}\text{Mg}_{42}\text{Ho}_8$  sample prepared under the same condition as Ref. [11]: the as-cast sample was annealed at 873 K for 20 min and subsequently at 673 K for 48 h. Shown in Fig. 1 is the backscattered electron image taken in SEM. It clearly shows the coexisting four phases as i-QC,  $(\text{Zn}_{1-x}\text{Mg}_x)_5\text{Ho}$ ,  $\text{Zn}_3\text{Mg}_7$ , and Mg. The i-QC was shown to have a composition of  $\text{Zn}_{57}\text{Mg}_{33}\text{Ho}_{10}$ , which is almost the same as the stoichiometric composition. The last two phases are nonmagnetic crystalline phases. In addition, there remains the magnetic  $(\text{Zn}_{1-x}\text{Mg}_x)_5\text{Ho}$  phase with  $x \sim 0.2$ . Further anneal reduces this phase; however, we found that a very long time is required to completely eliminate it in the Ho system. Thus, the previous diffraction pattern can possibly be a superposition of the magnetic signals from  $(\text{Zn}_{1-x}\text{Mg}_x)_5\text{Ho}$  and i-QC.

Having the above metallographic knowledge in mind, we made a  $\text{Zn}_{60}\text{Mg}_{30}\text{Ho}_{10}$  sample annealed at 723 K for 200 h. The SEM result showed that 90% or more of the sample is i-phase. Thus, by comparing it with the  $\text{Zn}_{50}\text{Mg}_{42}\text{Ho}_8$  sample, we regard it as an almost single i-phased sample. The powder diffraction pattern of this sample is shown in Fig. 2(a). The scattering intensity,  $I(|\vec{Q}|)$ , taken at  $T = 20$  K is shown as a high-temperature reference with only nuclear Bragg peaks. The peaks could be indexed with six indices, confirming the quasiperiodic nature of the sample. The 6D lattice constant was estimated as  $a_{6D} \approx 14.6 \text{ \AA}$ . Development of magnetic scattering intensity at the low temperature of  $T = 1.6$  K is displayed by a subtraction, i.e.,  $I(T = 1.6 \text{ K}) - I(T = 20 \text{ K})$ . Although the temperature is well below  $T_N \approx 7$  K, there appears to be almost no magnetic Bragg peak, indicating the absence of the LRO in the single-phased sample. In contrast, broad peaks appear at  $|\vec{Q}| \sim 0.55, 1.15, \text{ and } 2.0 \text{ \AA}^{-1}$  and reproduce the SRO part of the previous Letter.

The powder diffraction pattern of the  $(\text{Zn}_{1-x}\text{Mg}_x)_5\text{Ho}$  sample is shown in Fig. 2(b) with using the same manner as Fig. 2(a). We selected  $x = 0.2$  and annealed at 1023 K for 1 h and then at 923 K for 20 h to obtain a single-phased sample. The nuclear Bragg peaks can be indexed with

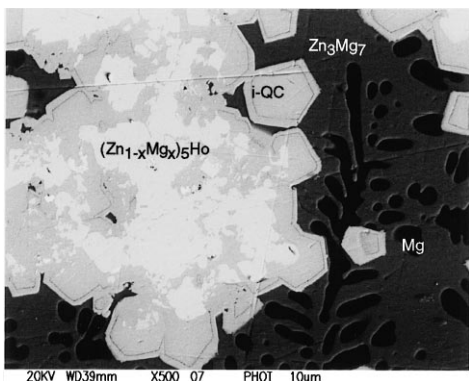


FIG. 1. The backscattered electron image of the  $\text{Zn}_{50}\text{Mg}_{42}\text{Ho}_8$  sample prepared under the same condition as Ref. [11].

hexagonal  $\text{Zn}_5\text{Ho}$  structure using the lattice parameters of  $a = 8.93 \text{ \AA}$  and  $c = 9.32 \text{ \AA}$  [14]. At low temperatures, magnetic Bragg peaks appear at the same positions as the intense LRO peaks in the previous Letter. They were indexed with quasiperiodic indices. However, this should be misleading indexing, since they apparently originate from the crystalline phase. The ordering temperature was determined by measuring magnetic susceptibility as  $T_N \approx 7.4$  K [15], which is almost equal to that of the previously reported LRO. The above results strongly suggest that the intrinsic magnetism in i-QC is SRO and that the previously reported LRO can probably arise from the crystalline phase.

Next, we investigated the  $\vec{Q}$  dependence of the diffuse scattering using the single crystal. Shown in Fig. 3 are results of  $\vec{Q}$  scans along the 2f, 3f, and 5f axes. Scans at two temperatures  $T = 1.3$  and 20 K were performed and results are shown in the same manner as the powder results. At  $T = 20$  K, well-indexed nuclear Bragg reflections were observed, confirming the single crystallinity of the sample. At  $T = 1.3$  K, the diffuse scattering evolves as observed in the powder sample, however, in a highly anisotropic form as follows. Magnetic intensity along the 2f axis exhibits well-developed diffuse peaks, indicating the existence of the short-range spin correlations. The

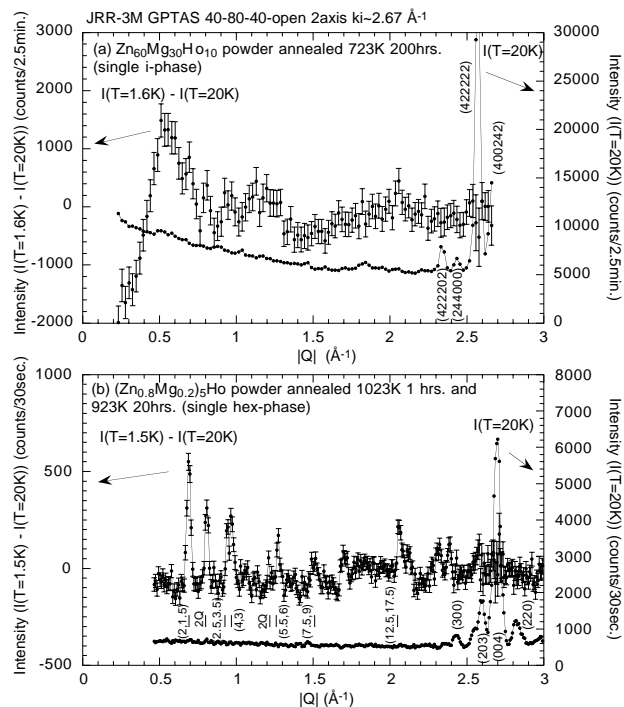


FIG. 2. (a) The powder diffraction pattern of the  $\text{Zn}_{60}\text{Mg}_{30}\text{Ho}_{10}$  i-QC. The result at  $T = 20$  K and the difference between 20 and 1.6 K are shown. The suffix “6D” of indices is ignored for simplicity. (b) The powder diffraction pattern of the  $(\text{Zn}_{0.8}\text{Mg}_{0.2})_5\text{Ho}$  crystalline phase, shown in the same manner as (a). The vertical lines represent the intense LRO peak positions in the previous Letter with the proposed QC indices [8]. Note that the magnetic Bragg peaks apparently originate from the crystalline phase.

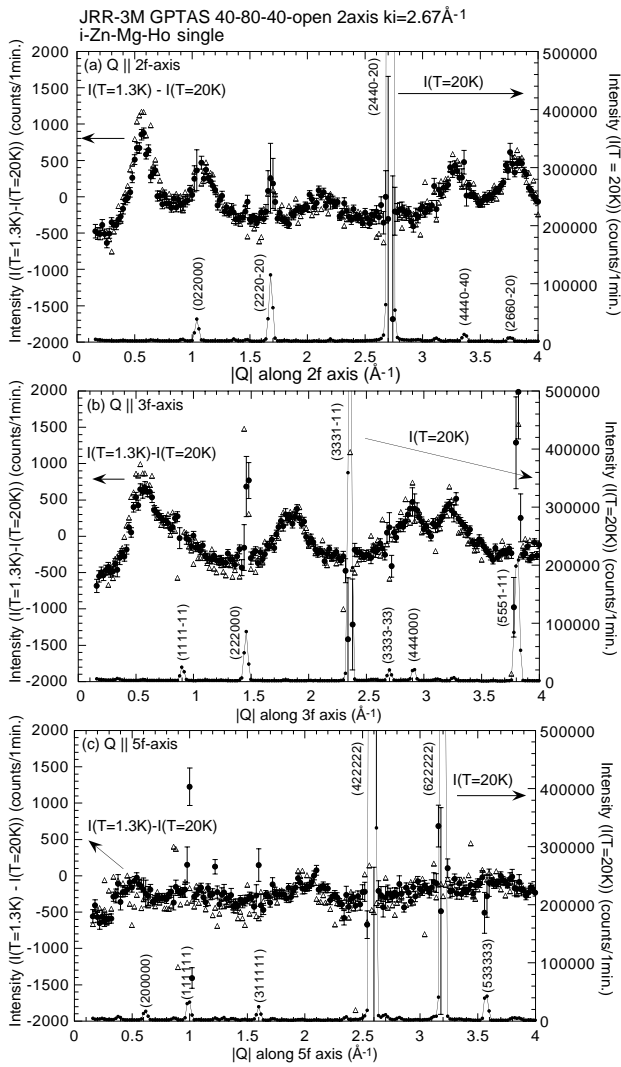


FIG. 3. The  $\vec{Q}$  scans along the (a) 2f, (b) 3f, and (c) 5f axes in the Zn-Mg-Ho single i-QC, shown in the same manner as the powder result. Triangles and dots for the differences stand for the data along two symmetrically equivalent directions, such as  $\vec{Q} = (Q_x, 0, 0)$  and  $(0, Q_y, 0)$  for the 2f axis. The suffix 6D of indices is ignored for simplicity.

correlation length was estimated as  $\xi \sim 10 \text{ \AA}$  from the peak at  $\vec{Q} \sim (0.55, 0, 0) \text{ \AA}^{-1}$ . Diffuse peaks could also be observed along the 3f axis with wider widths, and thus the correlation length becomes shorter in this direction. In contrast, almost no magnetic scattering could be observed along the 5f axis. This indicates very weak correlations along the 5f axis. Note that no magnetic Bragg peak appears in the scans. This confirms the absence of LRO in i-QC.

To see the overall features of the diffuse scattering in  $\vec{Q}$  space, we have made a magnetic-scattering intensity map. Since only the broad diffuse peaks appear at low temperatures, we employed the looser collimation of  $40' - 80' - 80'$  to gain intensity. Further, to achieve reasonable statistical accuracy within limited experiment time, we measured the intensity in the following procedure. First, half of the scat-

tering plane, i.e.,  $Q_x > 0$  and  $|\vec{Q}| < 4 \text{ \AA}^{-1}$ , was scanned at  $T = 1.3$  and 20 K. After confirming that the subtracted magnetic intensity satisfies the symmetry requirement, we folded the data into a single quadrant of  $Q_x, Q_y > 0$ . Finally, the quadrant was repeated for all the  $|\vec{Q}| < 4 \text{ \AA}^{-1}$  space to see characteristics of the intensity distribution.

Figure 4 shows the resulting intensity map of the magnetic contribution. A few intense spotlike peaks can be seen in the map. However, they do not correspond to magnetic Bragg reflections but are definitely diffuse scattering, as evidenced by the corresponding scans in Fig. 3. In the map, one can see ridges parallel to the 5f axis, which pass through the intense peaks. The ridges appear as satellites of intense nuclear Bragg reflections, such as  $\vec{O}_{6D} = (000000)_{6D}$ ,  $\vec{G}_{6D}^1 = (244020)_{6D}$ ,  $\vec{G}_{6D}^2 = (422222)_{6D}$ , and  $\vec{G}_{6D}^3 = (311111)_{6D}$ .

A position on the  $\vec{Q} = (Q_x, Q_y, 0)$  plane in 3D reciprocal space is projected from  $\vec{Q}_{6D} = (Q_1 Q_2 Q_2 Q_4 Q_5 Q_4)_{6D}$  by

$$\begin{pmatrix} Q_x \\ Q_y \end{pmatrix} = \alpha' \begin{pmatrix} Q_1 + 2\tau Q_2 - Q_5 \\ \tau Q_1 + 2Q_4 + \tau Q_5 \end{pmatrix}, \quad (1)$$

where  $\alpha' = (2\pi/a_{6D}\sqrt{2} + \tau)$  and  $\tau$  is the golden ratio [9]. Since it is a linear operation, the observed satellite ridges can also be assigned to corresponding satellite ridges of the form  $\vec{Q}_{6D} = \vec{G}_{6D} \pm \vec{q}_{6D}$  in the 6D reciprocal space, which have to be elongated along the 5f axis.

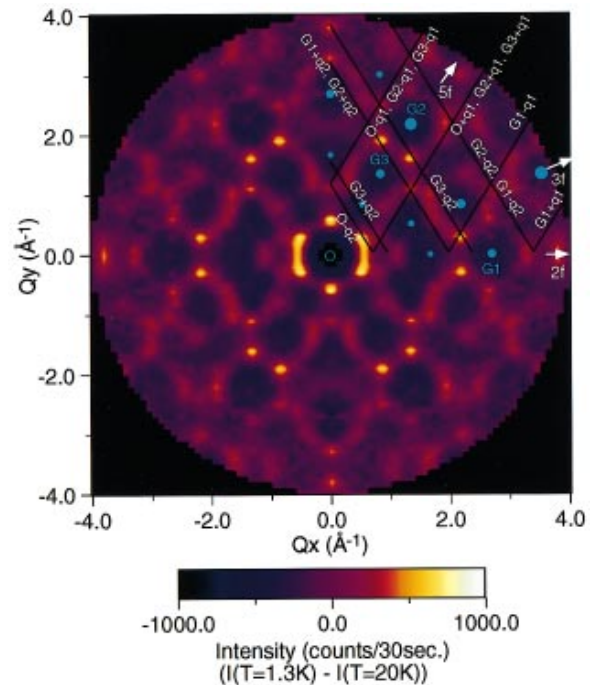


FIG. 4(color). The magnetic-scattering intensity map obtained by subtracting the data at  $T = 20$  K from those at 1.3 K. The blue dots denote the intense nuclear Bragg positions. The black lines are projected loci of the magnetic diffuse positions,  $\vec{G}_{6D}^m \pm \vec{q}_{6D}^n$ , where suffix 6D is ignored in the figure. They are drawn only in the first quadrant.

( $\vec{q}_{6D}$  is a magnetic wave vector.) Then the most simple  $\vec{q}_{6D}$  that reproduces the observed ridge positions is  $\vec{q}_{6D}^1 = (x11\bar{1}0\bar{1})_{6D}$  and  $\vec{q}_{6D}^2 = (0\bar{1}\bar{1}\bar{1}x\bar{1})_{6D}$ , with  $x$  being arbitrary. The projected loci of the ridges are shown in Fig. 4, for the intense Bragg reflections as  $\vec{O}_{6D}$ ,  $\vec{G}_{6D}^1$ ,  $\vec{G}_{6D}^2$ , and  $\vec{G}_{6D}^3$ . They reproduce well the observed ridges as a first approximation. This strongly suggests that the wave vector of the diffuse scattering should be defined in the 6D reciprocal space. The diffuse scattering is positioned at forbidden nuclear reflections, indicating antiferromagnetic spin coupling. Further, since it is elongated along the 5f axis, the spin correlations can be regarded as *quasi-five-dimensional* in the 6D space.

In the above discussion, we did not take account of intensity. The intensity of the projected reflection, generally, decreases for large  $|\vec{Q}_\perp|$ , where  $\vec{Q}_\perp$  is the projection of  $\vec{Q}_{6D}$  into the 3D complementary space, orthogonal to the 3D physical  $\vec{Q}$  (reciprocal) space [9]. The intense Bragg reflections have apparently small  $|\vec{G}_\perp|$ , and thus the satellites of them also have small  $|\vec{Q}_\perp| = |\vec{G}_\perp \pm \vec{q}_\perp|$ , for small  $x$ , and will appear in observation. This explains why only the satellite ridges around intense Bragg reflections can be observed and may also reproduce the spotlike behavior since the spotlike peaks appear at positions closest to the corresponding Bragg positions on the ridges. The ridges can still continuously appear along the 5f direction in the 3D reciprocal space, since there are several Bragg reflections along this axis, such as  $\vec{G}_{6D}^2$  and  $\vec{G}_{6D}^3$ . Qualitative discussion is left for further study because it requires the precise coordinate of the RE sites. The structure determination is now in progress [16].

The present study shows that highly anisotropic spin correlations develop at low temperatures, whereas the magnetic susceptibility in the single-phased sample exhibits the spin-glass-like behavior [15]. Thus, the spins should freeze at low temperatures with the well-developed short-range correlations characterized by the quasiperiodic  $\vec{Q}$  vector. This frozen state is quite unique among ordinary spin glasses, where, even if the correlations develop, corresponding diffuse scattering is generally weak and appears periodically in  $\vec{Q}$  space. The key to understand the frozen state may be found in the self-similarity intrinsic to the quasiperiodicity. A very simple Ising-model with a self-similar structure was studied and shows a nonclassical spin-glass transition with strong spin correlations in a chaotic sequence [17]. Although the model is too simple and not realistic, the existence of the spin-glass-like state with aperiodic spin correlations suggests that it may give a starting point to understand the frozen state of Zn-Mg-Ho i-QC.

In conclusion, we have observed highly anisotropic magnetic-diffuse scattering in the Zn-Mg-Ho icosahedral quasicrystal. The previously reported long-range order could not be detected in the icosahedral phase. The  $\vec{Q}$  dependence of the diffuse scattering suggests that the quasi-five-dimensional spin correlations develop in the

six-dimensional lattice. Further study, both theoretically and experimentally, is obviously required to elucidate the nature of the spin correlations and relation with the spin-glass-like behavior observed in magnetic susceptibility.

The authors thank B. Charrier and T. Ishimasa for providing us the results prior to publication, and H. Yoshizawa for a critical reading of the manuscript. Valuable discussions with E. Abe, K. Nakajima, H. Kadowaki, M. Nishi, and M. Kohgi are acknowledged. This work is partly supported by CREST, Japan Science and Technology Corporation.

*Note added.*—Recently, a related paper which reports the absence of the long-range magnetic ordering in the Zn-Mg-Tb icosahedral quasicrystal has been published [18].

- 
- [1] For a review, A. Yamamoto, *Acta Crystallogr. Sect. A* **52**, 509 (1996).
  - [2] C. Janot, *Quasicrystals, a Primer* (Clarendon Press, Oxford, 1992).
  - [3] A. P. Tsai, A. Inoue, Y. Yokoyama, and T. Masumoto, *Mater. Trans. JIM* **31**, 98 (1990).
  - [4] B. Dubost, J. M. Lang, M. Tanaka, P. Sainfort, and M. Audier, *Nature (London)* **324**, 48 (1986).
  - [5] S. Takeuchi, H. Akiyama, N. Naito, T. Shibuya, T. Hashimoto, K. Edagawa, and K. Kimura, *J. Non-Cryst. Solids* **153&154**, 353 (1993).
  - [6] M. de Boissieu, M. Boudard, R. Bellissent, M. Quilichini, B. Hennions, R. Currat, A. I. Goldman, and C. Janot, *J. Phys. Condens. Matter* **5**, 4945 (1993).
  - [7] Z. Luo, S. Zhang, Y. Tang, and D. Zhao, *Scr. Metall. Mater.* **28**, 1513 (1993).
  - [8] B. Charrier, B. Ouladdiaf, and D. Schmitt, *Phys. Rev. Lett.* **78**, 4637 (1997). The  $\vec{q}_{6D}$  vector in this paper corresponds to  $(\frac{1}{2}00000)$  with the present definition [9].
  - [9] Throughout this Letter, the Elser's definition of indexing is used with body-centered hypercubic reciprocal lattice: V. Elser, *Phys. Rev. B* **32**, 4892 (1985). The bases of 6D lattice, presently used, are given by A. Yamamoto, *Phys. Rev. B* **45**, 5217 (1992), with slight difference: present  $a_{6D}$  corresponds to  $\sqrt{2}a$  in the paper.
  - [10] Y. Hattori, A. Niikura, A. P. Tsai, A. Inoue, T. Masumoto, K. Fukamichi, H. Aruga-Katori, and T. Goto, *J. Phys. Condens. Matter* **7**, 2313 (1995).
  - [11] B. Charrier and D. Schmitt, *J. Magn. Magn. Mater.* **171**, 106 (1997).
  - [12] A. P. Tsai, A. Niikura, A. Inoue, and T. Masumoto, *J. Mater. Res.* **12**, 1468 (1997); A. Langsdorf, F. Ritter, and W. Assmus, *Philos. Mag. Lett.* **75**, 381 (1997).
  - [13] T. J. Sato, H. Takakura, and A. P. Tsai, *Jpn. J. Appl. Phys.* **37**, L663 (1998).
  - [14] M. L. Fornasini, *J. Less-Common Met.* **25**, 329 (1971).
  - [15] T. J. Sato *et al.* (to be published).
  - [16] H. Takakura *et al.* (to be published).
  - [17] S. R. McKay, A. N. Berker, and S. Kirkpatrick, *Phys. Rev. Lett.* **48**, 767 (1982).
  - [18] Z. Islam, I. R. Fisher, J. Zarestky, P. C. Canfield, C. Stassis, and A. I. Goldman, *Phys. Rev. B* **57**, R11047 (1998).